

# **Slow slip and locking at the Hikurangi subduction zone, New Zealand, inferred from time-dependent inversion of three-component continuous GPS**

Robert McCaffrey and John Beavan

GNS Science, Lower Hutt, New Zealand

## **SUMMARY**

The Hikurangi subduction zone offshore the North Island, New Zealand, has produced slow slip events at a variety of depths and durations. We invert six years of 3-component continuous GPS time series at 50 sites for the source parameters of the slow-slip events (SSEs) and also estimate the locking on the subduction zone in the time between events. Several SSEs occurred at shallow levels (< 15 km) of the fault and a few were deeper (> 30 km). The shallow events are generally of short duration (less than tens of days) while the deep ones last up to a year, a trend opposite to that seen in Japanese slow-slip events. The shallow slow slip occurred where fault temperatures are low, well outside the commonly accepted range for the frictional stability transition. Over the 6-year time period sampled, slow slip released about one-third of the accumulating strain on the plate boundary and there is earlier geodetic evidence that this fraction may vary with time. A signal that we interpret as accelerated locking over several months is seen immediately following some shallow events, suggesting that the plate boundary is not always fully locked and re-loading in the time between events. Despite the great variation in depths of the SSEs, we find that they all occur at the base of the geodetic transition zone suggesting that the geodetic transition zone coincides with the frictional stability transition.

## **1. Introduction**

Slow-slip events (SSE) are thought to be due to slip on fault planes, much like earthquakes, but occur slowly enough to not radiate detectable seismic waves. The role of such slow, aseismic slip in

accommodating fault movement is just starting to be understood particularly with regard to its impacts on great earthquake occurrence. While most slow slip at subduction zones has been observed at or below the transition zone (Schwartz and Rokosky, 2007), where frictional properties go from unstable (slick-slip, or velocity-weakening) to stable sliding (free-slip, or velocity-strengthening), largely temperature-dependent, slow slip at the Hikurangi subduction zone off North Island, New Zealand, is unusual in that most events occur at shallow parts of the thrust fault where temperatures are relatively low (McCaffrey et al., 2008). The role of slow slip in moderating the temporal and spatial release of seismic energy from the fault is critical for understanding their impact on earthquake hazards forecasting. Here we investigate the slip distributions of the slow slip along the Hikurangi subduction thrust by direct inversion of the GPS time series.

The Pacific plate subducts westward beneath Australia at the Hikurangi margin (Fig. 1a). The rate is about 45 mm/yr in the north and decreases toward the south (Beavan et al., 2002). Due to the curvature of the deformation front, the obliquity of the relative motion increases southward and the amount of convergence decreases as shear increases. In the northern South Island, relative motion is nearly all shearing across the Marlborough fault system (Holt and Haines, 1995; Wallace et al., 2006). The incoming Pacific plate is old, probably Cretaceous in age (Mortimer and Parkinson, 1996), and hence the Hikurangi subduction fault is relatively cold (McCaffrey et al., 2008).

Deformation around the Hikurangi margin is complex, driven not only by the Pacific convergence obliquity but also includes backarc extension at the Taupo volcanic zone (TVZ; Wilson et al., 1995; Villamor and Berryman, 2000). The forearc comprises several separate crustal blocks that rotate clockwise relative to Australia (Wellman, 1974; Beanland and Haines 1998; Walcott, 1978; 1984; Wallace et al., 2004). Upper plate strike-slip and normal faults partition the slip across the North Island such that a large fraction of the relative motion is by upper plate deformation. Using 12 years (1991-2003) of survey-mode GPS (sGPS) measurements and geologic

fault slip rates, Wallace et al. (2004) quantified the rotations of crustal blocks and fault slip rates. In addition to confirming the block rotations first suggested from paleomagnetism and geology, that work also revealed that the depth of locking on the Hikurangi plate interface varies greatly along strike, from < 20 km in the north to ~ 60 km in the south, with a sharp lateral transition around 40°S. The question remains whether or not the 12 years of GPS observations provide a representative snapshot of the entire great earthquake cycle that is likely to be hundreds of years. The past few decades of seismicity support such a locking distribution over longer time frames (Reyners, 1998).

Continuously operating GPS (cGPS) sites were started in New Zealand in the early 2000s (Fig. 1b) and have since recorded several slow slip events (Douglas et al., 2005; Wallace and Beavan, 2006; Beavan et al., 2007). The SSEs are not nearly as regular as in Cascadia, for example, but do seem to repeat in the same general parts of the fault interface. Hence, it is reasonable to assume that some undetected SSEs occurred in the years of the sGPS surveys. In addition it is likely that, due to their temporal irregularity, the slip in the SSEs that occurred in 1991-2003 were not representative of the long-term slip in SSEs. Accordingly, it is likely that the site velocities estimated from the sGPS are neither the velocities of the sites between such transients nor the long term (several decade or longer) velocities. Such ambiguity in the surface velocity estimates leads to biased estimates of the parameters of the physical model used. The necessity of separating the long term linear motion from the transients in part motivates this work. We test whether or not the site velocities between transients are constant through time.

The goals of this work are (1) to characterize the slow slip events at the Hikurangi margin and (2) to estimate the site velocities in the period between transients. We find that, with a few exceptions, the site velocities between transients are constant, that is, the velocity before and after transients is in general quite similar. In some cases, the velocity is faster in the months following

slow slip, suggesting that the fault is re-loading at an accelerated rate. We model the locking of the plate interface based on the corrected site velocities which reveals a very close relationship between the geodetic transition zone (where interseismic locking dies out at depth) and the locations of the SSEs. This region of the fault is likely marking the frictional stability transition zone and, if so, may be where rapid slip in earthquakes dies out at depth.

## 2. Method

### 2.1 Linear motions

As continuously operating GPS sites become more numerous, methods to quickly and automatically interpret their time series are required. We present a method to invert the time series to estimate the long term linear motions of sites and short-term transients such as slow slip events, volcanic sources and earthquakes. The approach we take is an expansion of the method developed by McCaffrey (1995; 2002). The long-term constant geodetic surface velocities are viewed as a combination of crustal block rotations, elastic strain rates from locked faults and distributed permanent strain rates. Here that part of the problem is represented by a linear time series of discrete observations of position  $X$ :

$$X_{ij}(t) = X_{ij}^0 + V_{ij} ( t - t_o ) \quad (1)$$

where  $X_{ij}^0$  is the initial position of component  $i$  (east, north and up) of site  $j$  at time  $t = t_o$  and  $V_{ij}$  is the  $i^{\text{th}}$  component of secular velocity of site  $j$ . The velocity  $V$  is estimated by finding the slope of each component of each site simultaneously with the parameters describing the transient sources.

### 2.2 Transient motions

The main type of transient to be addressed is slow slip on the Hikurangi subduction fault but the method can also be applied to earthquakes (with afterslip) and time-dependent volcanic sources.

Inversions have generally solved for slip on patches of the fault and used smoothing (regularization) to specify the covariance between adjacent and nearby patches that are usually not independently resolved (e.g., Segall and Matthews, 1997; Fukuda et al., 2008). Here, we describe the slip during the transient event by a simple Gaussian function of position and time which allows it to be described with a small number of free parameters. In its simplest, we describe the slip on the fault during the event by:

$$s(x, w, t) = A \exp(-\frac{1}{2} [(x-X_c)/X_s]^2) \exp(-\frac{1}{2} [(w-W_c)/W_s]^2) \exp(-\frac{1}{2} [(t-T_c)/T_s]^2) \quad (2)$$

where  $s$  is the slip rate on the fault at along-strike position  $x$ , down-dip position  $w$  and time  $t$ ,  $A$  is the amplitude,  $X_c$  is the along-strike center of the slip function and  $X_s$  represents its along-strike spread,  $W_c$  and  $W_s$  are the down-dip center and spread, and  $T_c$  and  $T_s$  are the temporal center and spread. For a slow slip event the seven free parameters  $A$ ,  $X_c$ ,  $X_s$ ,  $W_c$ ,  $W_s$ ,  $T_c$  and  $T_s$  describe the slip distribution ( $A$  is given in mm/yr,  $X_c$  and  $W_c$  are in km but converted to degrees of longitude and latitude,  $X_s$  and  $W_s$  are in km,  $T_c$  and  $T_s$  in years). The surface displacement history is found by integrating (2) over time (Fig. 2) and applying the appropriate Green's functions. The start time of the slow slip is given as  $T_c - 2T_s$  and its duration is defined as  $4T_s$ ; the time it takes for 95% of the slip to occur.

To account for migration of the slip sources, as is seen in Cascadia (Dragert et al., 2004), the time function is delayed or advanced in time relative to  $T_c$  depending on the migration rate and direction. We tested for migration of slip in New Zealand SSEs but did not find any resolvable motion. Equation (2) can also be used to represent distributed slip during an earthquake on the fault by fixing  $T_c$  to the origin time of the earthquake and  $T_s$  to a small value (a small fraction of the

temporal sampling interval) which results in a spike in the slip rate (in time) and a step in displacement.

The term  $A \exp(-\frac{1}{2} [(t - T_c)/T_s]^2)$  in (2) controls the moment rate of the slip event in our parameterization (where the other two independent terms give the slip area). It has been suggested that the equivalent moment (rigidity times area times slip amount) for slow-slip events scales proportionally with event duration (Schwartz and Rokosky, 2007) with a ratio of moment to duration of  $10^{-12}$  to  $10^{-13}$  N-m/s (Ide et al., 2007). This suggests that moment rate is approximately constant and that the frequency ( $f$ ) spectrum should decay as  $f^1$  and not as  $f^2$  as in regular earthquakes. A constant moment rate is represented by a box-car slip-rate history (for constant slip area) which results in a linear displacement history at the surface sites. We attempted to fit the GPS time series using box-car time histories (amplitude and duration as free parameters) but this gave a poor fit to the long-duration events. The clear S-shaped curvature of the surface displacement histories (see site TAKP in Fig. 3 for example) cannot be matched by a constant moment rate source. The time dependence can also be described using multiple, over-lapping triangular source time elements, that reproduce the curvature in the displacement histories, but this introduces more free parameters and in general produces Gaussian-looking time histories. We find that the Gaussian time function, with only two free parameters, is sufficient for Hikurangi events described here.

Following some slow-slip events we noted a faster site velocity directed opposite the sense of slip in the SSE (Fig. 3). We interpret these as re-locking of the fault at a rate faster than normal. To model this feature in the times series we parameterize it by a constant locking velocity  $V_l$  that starts near the end of the SSE (at  $t = T_c + 3T_s$ ) and lasts a time  $T_l$  (Fig. 2). We assume that the re-loading occurs over the same patch of fault that slipped during the preceding SSE.

## 2.3 GPS data

The primary data used are the daily positions of continuous GPS sites in the North Island and northernmost South Island, above the Hikurangi subduction zone from 2002 until the end of 2007. Some sites have been operating since 2000 but many more were installed since 2003 as part of the GeoNet project (ref). Hence, the sampling varies greatly through the time investigated. Daily positions are estimated in the ITRF2000 reference frame with Bernese (Rothacher and Mervart, 1996) and a common mode correction is made. The time series are rotated into the Australian reference frame using the Australian ITRF pole of Beavan et al. (2002). Each position is assigned an uncertainty (1.5 mm for the east and north, 5.0 mm for the vertical). Here we use the average 2-day positions. After finding a solution, we culled the data by removing outliers whose normalized residuals exceeded four, and then re-inverted the data. Only a few hundred out of about 80,000 data were removed in this way.

## 2.4 Physical Model

The three-dimensional Hikurangi slab geometry is based on seismicity (Ansell and Bannister, 1996) and is digitized by specifying nodes approximately every 15 km along strike and downdip. The surface response to distributed slip on the fault is obtained by first calculating the response at each node (Green's functions; see McCaffrey, 2002), then convolving the Green's functions with the slip distribution (equation 2) as evaluated at the nodes. Response functions are derived for an elastic halfspace using the formulation of Okada (1995) and the method described by McCaffrey (2002).

The subduction vectors are derived from the block angular velocities of Wallace et al. (2004) and the slow slip events are assumed to be due to slip on the subduction zone fault in the opposite direction. We find that for the most part the data are consistent with this assumption of slow slip

opposite the local subduction direction and hence do not solve independently for the slip direction during the events.

## 2.5 Inversion

The best-fitting parameters are estimated by minimizing the sum of the squares of the weighted residuals plus any penalties due to parameter constraints, such as forcing positivity in some slip parameters. The goodness-of-fit criterion is the reduced chi-square statistic:

$$\chi_r^2 = (N-P)^{-1} \sum_{i=1,N} (r_i/\sigma_i)^2$$

where  $N$  is the number of data,  $P$  is the number of free parameters,  $r_i$  is the residual of the  $i^{\text{th}}$  datum and  $\sigma_i$  is its standard error. The inversion was done in two steps. First each transient was analyzed separately using a short bracketing section of the time series while estimating linear trends of each site-component independently. After obtaining preliminary estimates of the parameters for each transient, we inverted for all the transients using the entire time series again allowing the long-term secular velocities to be independent. For the final runs,  $N \sim 72,500$ ,  $P = 339$ , and  $\chi^2 \sim 0.84$ . Uncertainties were estimated at the end by forming the parameter covariance matrix assuming a linear system of equations.

## 3. Results

### 3.1 Transient events

Events that caused the GPS time series to deviate from linearity comprised 12 slow slip events on the Hikurangi thrust. There were four small excursions seen at site TAUP, near the Taupo caldera within the Taupo volcanic zone (TVZ), but these are likely due to local volcanic events and are not modeled (only the latest of these, in late 2007, appears to have moved more than one site and is consistent with a volcanic expansion event). Each event has up to 7 free parameters. Two of

them, the temporal parameters,  $T_c$  and  $T_s$ , can be estimated with a single time series. The remaining 4 spatial parameters,  $X_c$ ,  $X_s$ ,  $W_c$ ,  $W_s$ , and the amplitude  $A$  require multiple sites. Each site provides 3 spatial observations – *i.e.*, the displacements in each of the 3 components. Hence at least 2 sites with observable displacements are needed to estimate the parameters. Early events are poorly mapped due to a paucity of operating sites. For those events we fix a number of parameters at reasonable values and solve for the others. In some cases we force events that look similar to have the same parameter values; for example three events that moved only one site were set to have the same position and slip extents. Finally, we correct for the 2004 Macquarie earthquake that visibly displaced most of the sites by up to 2 mm by solving for east, north and up offsets common to all sites.

Here we discuss the individual events by region (denoted by Event number). Parameters are given in Table 1. Maps of some events are shown in Fig. 4 and the rest are in the Supplemental Material.

**3.1.1 Gisborne region** (Events 1, 3, 8, 9, 10, 12). Event 1 was reported on by Douglas et al. (2005) and was recorded by only 2 nearby GPS sites. The next closest operating site, HAST, was 150 km distant and did not appear to be displaced in any component. We fixed the slip rate amplitude  $A = 400$  mm/yr (maximum surface displacement ~35 mm) and solved for the remaining six parameters. Douglas et al. (2005) show that the observed down in the verticals constrains the source to be offshore (in general, sites on the updip side of the slip region go up, sites downdip go down). The predicted displacement at HAST is at most ~1 mm suggesting that for any larger moment or if the event were any farther south (closer to HAST), it would have been observed there. The large gradient in displacements at the two sites near Gisborne suggests it is very close by. The moment is  $1.49 \times 10^{19}$  Nm ( $M_w = 6.7$ ).

The large Event 8 in 2004 ( $M_w = 6.57$ ) was recorded at only two sites (GISB and MATW) while KOKO was just coming on-line. Event 12 occurred in the same area and detected by 3 sites. An offshore source is suggested by subsidence at coastal site GISSB and larger amplitudes than at inland MATW. Three small events (3, 9, and 10) were observed at the KOKO or GISSB or both sites but could not be modeled well. For these we set the location to be the same as Event 8 and solved for the remaining parameters.

**3.1.2 Kapiti region.** Event 2 was a deep, long-duration event reported by Beavan et al. (2007), based on movement at one site, PAEK. The time series inversion suggests that two other sites, WGTN and MAST, may have moved by a few mm during the event. The source duration was about one year and the moment is  $2.2 \times 10^{19}$  Nm ( $M_w = 6.8$ ). A similar event started in late 2007 and was continuing at the time of this writing.

**3.1.3. Hastings.** Events 11 and 13 occurred a few months apart but were of short duration and did not overlap in time. They were very close together in space. Both events moved several sites in the dense network around Hastings and the pattern of motions places them both offshore. Two more earlier events (4 and 6) are postulated on the basis of the east (~6 mm) and north (~2 mm) offsets at one site, HAST (Beavan et al. 2007), that have the characteristics of the later, well-recorded offshore events. The vertical motions at HAST are ambiguous but the lack of displacement at the site RIPA, west of HAST, during Event 6 suggests the slip was east of HAST (RIPA was not operating during event 4). For events 4 and 6, we fixed all parameters ( $A = 60$  mm/yr) except the latitude and the two time parameters. The estimated moment for the two small events is  $3.0 \times 10^{18}$  Nm ( $M_w = 6.3$ ).

**3.1.4. Manawatu** Events 5 and 7 are two subevents of a long-duration, deep slip event reported on by Wallace and Beavan (2006). We have split it into two separate events based on an abrupt increase in slope of the time series in late 2004. By the time of this event, GPS coverage was quite

good and it was recorded by seven sites with greater than 5 mm amplitude (Fig 4). When treated as separate events, their estimated locations differ by about 30 km; when forced to have the same location the fit was only slightly worse. We cannot rule out that slip was stationary in space but had an accelerated slip phase late in 2004.

### **3.2 Migration of transients**

Transients in Cascadia are seen to migrate along the margin at rates of several km per day, both unilaterally and bilaterally (Dragert et al., 2004). In the New Zealand events, there is little obvious visible evidence of migration in the time series. Possible examples are events 8 and 12, both with large amplitudes at GISB (Fig. 3). At site KOKO, only 50 km from GISB, event 8 appears to be later by about a month (near the time this site started) and event 12 may be a few days early. We looked at the possibility of migration by allowing uni-directional migration with the migration rate and direction as free parameters in the inversions. None of the results were compelling.

### **3.3 Inter-event site velocities**

The velocities of the sites during the time intervals between transients are due to the steady strain accumulation on faults and crustal rotations within the relevant reference frame. In addition to the parameters describing the transient events, the inversion provides estimates of these long-term steady site velocities (Table A1). Velocity uncertainties were taken from the covariance matrix and a random walk component was added, using a factor of 1.0 mm/√yr (Mao et al., 1999).

The degree to which the velocities are constant over the time period can be seen in the plots of position residuals (Supplemental Material). In most cases the residuals fall within the range of uncertainties but there are some exceptions. For three events, we accounted for apparent changes in the post-event site velocity by allowing re-locking at a rate above the background rate. This effect

was largely seen at the northern sites GISB and KOKO near Gisborne (although KOKO does not have a well-determined long-term site velocity).

In addition to the transient-corrected velocities, we examine the impact of the transients on the estimated velocities by performing weighted linear regressions to the time series without correcting for transients. This simulates the velocities that might be obtained from intermittent campaign observations, for example, in which the site's motion is assumed to be linear in time. The comparison (Fig. 6a) reveals that the transients produce changes in the velocities at the level of several mm/yr. Comparing the velocities also to campaign-derived velocities from 1992-2003 reveals an even larger difference, suggesting that the difference depends on the time span examined. Arnadottir et al (1999) showed that in the region of the Raukamura Peninsula, surface strain rates are variable at the time scale of several decades, inferring that the locking on the thrust fault extended about twice as deep from 1976-1995 as it does now.

### 3.4 Inter-event Hikurangi locking model

The corrected inter-event velocities at the cGPS sites are used to estimate the locking distribution on the Hikurangi subduction fault. The procedure is similar to that followed by Wallace et al. (2004) but we use a different parameterization for the locking (see below) and apply along-strike smoothing to the locking distribution due to the limited number of continuous sites available. Like Wallace et al. (2004), we simultaneously solve for the rotations of a number of forearc blocks.

The parameterization of the locking distribution is based on the concept of the ‘effective transition zone’ (Wang et al., 2003). In this representation, the plate boundary is fully locked from the seafloor to a depth  $Z_1$  and then locking decays with depth following a smooth exponential function with one free parameter, the shape parameter  $\gamma$ , and then goes to zero below a second depth  $Z_2$ . This allows for smoothly varying coupling between  $Z_1$  and  $Z_2$  (see McCaffrey et al. 2007 for more complete description). Thus along any profile down the plate interface the locking fraction

is described by  $\phi(\gamma, Z_1, Z_2)$  and the backslip vector is  $-\phi \mathbf{V}$  where  $\mathbf{V}$  is the slip vector between the subducting and overriding plates. The downdip profiles in the slab model are about 15 km apart along strike. Because the surface geodetic data cannot resolve such short-wavelength features, we apply along-strike damping by limiting the change in  $\phi$  per unit distance.

The resulting locking distributions (Fig. 6b and 6c) reveal a very close relationship between the geodetic transition zone, where locking dies out at depth, and the locations of slow slip events. Slow-slip occurs at the downdip edge of the inter-event locking (Fig. 6c) but, for most of the margin, entirely downdip of the locked zone as imaged by the average velocities (Fig. 6b). This observation suggests that the slow-slip events are releasing the strain associated with the very base of the locked zone and that the locked zone may be extremely narrow if one exists at all.

Geodetic evidence suggests that the northern Hikurangi locked zone may change significantly at the decade or longer time scale. Arnadottir et al (1999) estimate that the fault was locked down to 30 km depth from 1976-1995 indicating significantly more coupling than today. Prior to that, from 1920-1976, the locked zone was shallower, perhaps by half (Arnadottir et al., 1999). The locked zone inferred from campaign data largely from the decade of the 1990's is different again (Wallace et al., 2004). The temporal irregularity and large moments of the slow slip events provides a simple explanation for the apparent changes in the locked zone using different time spans of geodetic data. If this is true, then it would be incorrect to infer earthquake potential from recent geodetic data. If Arnadottir et al. are correct that the fault was locked to 30 km (on average) over the previous two decades, then the more recent very shallow locking is not indicative of the amount of crustal strain that has accumulated and could be released in a large or great earthquake. As shown below, slow-slip from 2000-2007 released about one-third of the strain that accumulated during that period, as estimated with GPS.

The very shallow SSEs raise another interesting possibility to ponder – that the slow slip extends all the way to the deformation front. Clearly we have no control on the seaward extent of the slip. The symmetric Gaussian parameterization used results in the seaward edge of the slip distribution to be the mirror image of the landward edge which is constrained by the coastal GPS sites. If the slow slip extends all the way to the trench, then it suggests that there is no frictionally unstable section of the thrust fault at the present time. Unfortunately only frequent seafloor GPS could tell us whether or not slip continues to the deformation front.

## **4. Discussion**

### **4.1 Slow slip and the geodetic transition zone**

A clear feature of the Hikurangi slow slip events is their close association with the geodetic transition zone as described by surface geodetic data, an association that may be global (Schwartz and Rokosky, 2007). The Hikurangi margin is critical in understanding the relationship because both the slow slip and depth of the GTZ vary greatly along strike allowing examination of factors that may lead to these phenomena. Moreover, the change in the depth of the GTZ along strike rules out the many possible causes that would change only over large distances.

Models of the mechanics of slow slip generally find that they are expected to occur only within the frictional stability transition, where the frictional behavior of the fault goes from stick-slip (velocity weakening) at shallow depths to stable sliding (velocity strengthening) deeper along the interface. Hence the association of slow-slip with the geodetic transition zone, which may be interpreted as the stability transition, is not altogether unexpected. To date we have observed that slow-slip occurs within only a single depth range along any profile down the dip of subduction

interfaces. This suggests that whatever controls the conditions allowing slow slip is a single-valued function of depth.

Proposed controls on the location of the stability transition include composition, temperature, effective normal stress, and the presence or absence of gouge, fluids and hydrated minerals (e.g., Marone, 1998). We show elsewhere (McCaffrey et al., 2008) that temperature cannot be an important control, in general, for the Hikurangi margin. The very shallow (< 15 km) slow slip events offshore the northern Hikurangi margin, where Cretaceous ocean floor is being subducted, occur where fault temperatures are less than about 150°C. This is far below the range of temperatures (350°-450°C) expected for the stability transition based on laboratory experiments on granite (Blanpied et al., 1998) and on thermal and geodetic modeling of subduction zones (Hyndman and Wang 1993; Tichelaar and Ruff, 1993). Laboratory measurements on gabbro (He et al., 2007), which may be a better analog than granite for oceanic subduction settings, suggest that the transition temperature within subduction zones may be even higher, ~510°C.

Liu and Rice (2007) suggest that very low effective normal stress on the fault can allow slow slip instabilities that last on the order of months to years, similar to durations observed for most events in nature. (Higher effective stress leads to much longer duration events - we cannot rule out slow slip on the order of many years with our limited data to date.) However, their model requires that the slow slip occur within the stability transition zone which they place in the 350°-450°C temperature range for the reasons cited above. Segall et al. (2008) suggest that ‘dilatancy stabilization’ (Segall and Rice, 1995) can help explain the presence of slow slip outside the frictional transition zone, at low temperature for example. In this mechanism, slip that starts within an otherwise frictionally unstable section of the fault can be stabilized (resisted) by fluid pressure gradients that arise from changes in porosity accompanying slip. This mechanism can only be

important at very low effective stress where the pressure changes due to dilatancy are a significant fraction of the total effective stress.

Effective stress on faults is thought to be greatly reduced by the presence of fluids (water) that can be near lithostatic pressure. At shallow depths fluids are expelled from the sediments as they are compacted. Deeper, the oceanic crust gives up its water as porosity is reduced by pressure. At even greater depth, additional pressure can build from mineral dehydration reactions in the subducting lithosphere. Deeper slow-slip, in the 30-50 km depth range, could be responding to pore pressures from dehydration reactions but the shallower events are in the pressure range where dehydration is not occurring at fast rates. At shallow depths in northern Hikurangi, well data and mud volcanoes show that pore pressures are near lithostatic, probably from compression of the accretionary wedge and oceanic lithosphere (Allis et al., 1998; Sibson and Rowland, 2003).

However, dilatancy stabilization at shallow depths may be expected at all margins where shallow pore pressure is high, yet such shallow SSEs are rare. High pore pressures are seen in wells above the locked zone in the southern part of the Hikurangi subduction zone (Sibson and Rowland, 2003) where SSEs have occurred only along deeper parts of the fault. Furthermore, dilatancy stabilization, and other mechanisms involving high pore pressure, could possibly be active at more than one depth along a subduction fault, and we have yet to see SSEs (or tremor) at multiple depths along a single depth profile at any subduction zone. These observations suggest that whatever conditions allow slow slip or tremor or both to happen are reached only once in any depth profile along the faults.

## **4.2 Moment release in slow-slip**

The rate at which potential slip is accumulating is described by the so-called potency rate, which is the slip deficit rate integrated over the area of the fault (the potency rate is the moment rate divided

by the rigidity). For the model of inter-event locking (Fig. 6c) the potency rate is  $2.28 \times 10^9 \text{ m}^3/\text{yr}$ . The total moment released in slow-slip events is  $1.70 \times 10^{20} \text{ Nm}$  which gives a potency rate of  $7.1 \times 10^8 \text{ m}^3/\text{yr}$  (time is 6 years and rigidity  $\mu = 40 \text{ GPa}$ ). Hence the slow-slip events released over the 6 years 2002-2007 about 31% of the potential slip accumulation on the Hikurangi thrust. This is twice the relative slow-slip rate observed at Cascadia where about 10 to 15% of the moment is released in slow slip (McCaffrey et al., 2007). Globally, seismic moment release in earthquakes appears to account for about one-third of the expected moment at subduction zones based on fault slip rates and inferences about depth of plate friction (McCaffrey 1997, Frohlich & Wetzel, 2007). Slow slip may be a large part of this discrepancy as such events seem to be a common feature of subduction.

### 4.3 Source scaling and depth

A unique feature of the Hikurangi slow slip events is their very shallow depths. The slab contour is at about 15 km depth beneath the coast and most (10 of 13) events are seaward of the coast. Regardless of the uncertainties in their detailed locations, it is clear that they are shallower than 15 km. Only one well-recorded event (Manawatu sequence) and one suspected event (Kapiti, now confirmed by the ongoing slip event) are deeper than 15 km. This is in stark contrast to other subduction zones where the majority of SSEs are deeper than 30 km (Schwartz and Rokosky, 2007).

Another clear distinction we see is in the durations of slip. Shallow events are relatively short in duration (< 30 days) while the deep events last hundreds of days. At other subduction zones, both short and long deep events are observed at depth (Fig. 7). Beneath SW Japan, the deeper events ( $> 40 \text{ km}$ ) are short and small while the shallower events are larger and longer duration (Hirose and Obara, 2005). While the largest moment we observed at the Hikurangi margin was for a deep event,

there does not seem to be a trend in this respect. Moment rates range from  $10^{11}$  to  $10^{13}$  Nm/day which are typical rates (Ide et al., 2007).

Slow slip events have much smaller slip to fault length ratios than earthquakes (Brodsky and Mori, 2007). For earthquakes this ratio is about  $10^{-5}$  (Wells and Coppersmith, 1984) while it is roughly an order of magnitude smaller for slow slip events (Ide et al. 2007; Brodsky and Mori, 2007). New Zealand slow slip events show the same pattern (Table 1). Even though the shallow events have shorter durations, there is no obvious correlation of moment rate with depth for these events. The shallow slow slip events do not seem to follow the global trend of linear moment-duration but taken together with the deep events, there is a general increase in moment with duration (Fig. 7).

#### **4.4 Tremor and seismic activity**

High frequency, non-volcanic tremor is often but not always associated with slow slip events both in time and space (Schwartz and Rokosky, 2007). Sometimes tremor occurs in the absence of observable slow slip but the displacements may simply be too small to be recorded at the surface. Some small slip events, not seen in GPS, are inferred from sensitive tilt meters in Japan (Hirose and Obara, 2005). A large portion of the tremor energy downdip of the Nankai trough appears to be in the form of longer period (10s) shear failures (micro earthquakes) on the plate interface (Shelly et al., 2006). Such events are not seen in Cascadia (Kao et al., 2005; 2006) or in New Zealand (Delahaye et al., 2006). Moreover it is debated whether these events occur on the plate interface, as Shelly implies for Japan, or within the overriding plate, as Kao suggests for Cascadia. When tremor does occur along with observable slow slip, it typically releases only a fraction of the moment inferred from geodetic displacements (Houston, 2008).

In New Zealand, such tremor has not yet been identified despite careful scrutiny (Delahaye et al., 2006). However, possible examples of triggering of small, high frequency earthquakes have been found (Reyners and Bannister, 2007). In addition, the December 2007 Mw 6.8 normal-faulting earthquake offshore Gisborne appears to have triggered a large slow-slip event on the overlying thrust interface (unpublished results). The deeper slow-slip in New Zealand occurs at depths (30 – 50 km), depths at which other subduction zones are showing tremor. The causes of tremor are not at all understood so any guess as to why New Zealand does not produce it would be pure speculation. Currently, monitoring of slow slip and tremor are possible at only a few subduction zones so we should resist making correlations between the presence or lack of such phenomena with other properties of the subduction systems.

#### **4.5 Post SSE re-loading**

In the analysis of the GPS time series we assume that the site velocity over the observation time is a constant except as modified by slow slip events. For the vast majority of sites and components this appears to hold true. Occasionally we see velocities increase notably for a few months following the SSE (asterisks in Fig. 3), particularly near Gisborne. Although the GPS coverage there at the present time is sparse, the higher velocities appear only at sites that were displaced during the preceding slip event. That the faster velocities are not seen at the many sites that were not displaced during the SSEs suggests that it is a local effect and not widespread over the network. We modeled the faster velocities in the time series as due to increased locking (re-loading) following the SSE on the same patch of the fault that slipped. This gives an adequate fit to the time series but again the sparseness of the network does not allow a robust demonstration of the region of re-loading.

Two SSEs at Cascadia show a similar increase in velocity following slow slip (McCaffrey, 2008). The first one, in late 2000, was followed by about 400 days of velocity increases at several sites. The later one, in 2007, showed displacements and increased velocities at ~30 sites. This suggests that approximately the same region that slipped was subsequently re-loaded in the time following the slow slip.

Liu and Rice (2007) examined the impacts of both positive and negative small stress changes on slip velocity along a fault in the stability transition area. The positive stress changes led to slip velocity changes that are interpreted as slow slip while the negative stress perturbations led to slip in the opposite direction, that is, parallel to the subduction direction. For the 2000 Cascadia event a stress perturbation may have been produced by the Nisqually earthquake which occurred in Feb. 2001, a few weeks after the SSE stopped. The 2007 velocity increase does not have an obvious possible trigger. In the North Island, one of the velocity increases coincides with the Mw 8.1 Macquarie earthquake (Dec 2004) that produced visible offsets on the order of one mm at many sites of the network. However, this does not explain why only the sites near Gisborne had the velocity anomaly (many more sites should have changed velocity under the same trigger). In any case these faster velocities represent re-loading of the crustal strain although why they occur only intermittently is not clear.

## 5. Conclusions

Slow slip events have been observed at several subduction zones worldwide. It is thought that they occur within the zone of transition from stick-slip behavior (velocity weakening) to stable sliding (velocity strengthening). If so, they provide an observation to locate this transition zone at depth on the fault. At most subduction zones, the slow slip events occur at depths of greater than 30 km, presumably along the plate interface. At the Hikurangi trench in New Zealand, slow slip events

are seen within both the 30 – 50 km depth range and at less than 15 km. The shallow ones occur where fault temperatures are 150°C or less, calling into doubt the long-held dependence of the frictional transition zone on temperature. At the northern Hikurangi trench, where the shallow SSE occur, plate locking inferred from geodetic data changes dramatically depending on the time span examined. Such observations are revealing a very complex earthquake cycle with variability at many time scales and we should be hesitant in using the past few decades of geodetic observations as indicative of long-term processes.

**Acknowledgments.** Discussions with Jim Rice, Yajing Liu and Martin Reyners have been very helpful. Data courtesy of GeoNet (<http://www.geonet.org.nz>). Reviewed by ..... Supported by GNS Science, ...

## Citations

- Allis, R. G., R. Funnell and X. Zhan, From basins to mountains and back again: N.Z. basin evolution since 10 Ma, *Water-Rock Interaction*, Arehart and Hulston, eds., Balkema, Rotterdam, 3-9, 1998.
- Ansell, J. H., and Bannister, S. C., Shallow morphology of the subducted Pacific plate along the Hikurangi margin, New Zealand, *Phys.Earth Planet. Inter.*, **93**, 3 –20, (1996).
- Arnadottir, T., S. Thornley, S., Pollitz, F., and Darby, D., Spatial and temporal strain rate variations at the northern Hikurangi margin, New Zealand, *J. Geophys. Res.* **104**, 4931-4944 (1999).
- Beanland, S., and A. J. Haines, The kinematics of active deformation in the North Island, New Zealand, determined from geological strain rates, *N. Z. J. Geol. Geophys.*, **41**, 325-342, 1998.
- Beavan, J., Tregoning, P., Bevis, M., Kato, T., and Meertens, C., Motion and rigidity of the Pacific plate and implications for plate boundary deformation, *J. Geophys. Res.* **107**, 2261, doi:10.1029/2001JB000282, (2002).
- Beavan, J., Wallace, L., Douglas, A., Fletcher, H., and Townend, J., Slow slip events on the Hikurangi subduction interface, New Zealand, Dynamic Planet, Monitoring and Understanding a Dynamic Planet with Geodetic and Oceanographic Tools, IAG Symposium, Cairns, Australia, 22-26 August, 2005, Series: International Association of Geodesy Symposia , Tregoning, Paul; Rizos, Chris (Eds.), Vol. 130, 438-444, (2007).
- Blanpied, M. L., C. J. Marone, D. A. Lockner, J. D. Byerlee, and D. P. King, Quantitative measure of the variation in fault rheology due to fluid-rock interactions, *J. Geophys. Res.*, **103**, 9691–9712, 1998.
- Brodsky, E. E., and J. Mori, Creep events slip less than ordinary earthquakes, *Geophys. Res. Letts.* **34**, 34, L16309, doi:10.1029/2007GL030917, 2007.

- Delahaye, E. J., J. Townend, M. Reyners, M. P. Chadwick, (2006) Seismic tremor and small earthquakes associated with slow slip in the Hikurangi subduction zone, New Zealand, *Eos Trans. AGU*, 87(52), Fall Meet. Suppl., Abstract T41A-1548.
- Doser, D. I., and Webb, T. H., Source parameters of large historical (1917-1961) earthquakes, North Island, New Zealand. *Geophys. J. Int.* **152**, 795-832, (2003).
- Douglas, A., Beavan, J., Wallace, L., and Townend, J., Slow slip on the northern Hikurangi subduction interface, New Zealand, *Geophys. Res. Letts.* **32**, L16305, doi:10.1029/2005GL023607, (2005).
- Dragert, H., Wang, K., and James, T. S., 2001. A silent slip event on the deeper Cascadia subduction interface, *Science*, **292**, 1525-1528.
- Dragert, H., K. Wang, and G. Rogers, 2004. Geodetic and seismic signatures of episodic tremor and slip in the northern Cascadia subduction zone, *Earth Planets Space*, **56**, 1143-1150.
- Fukuda, J., S. Miyazaki, T. Higuchi, and T. Kato, 2008. Geodetic inversion for space-time distribution of fault slip with time-varying smoothing regularization, *Geophys J. Int.*, **173**, 25-48, doi:10.1111/j.1365-246X.2007.03722.x.
- He, C., Z. Wang, W. Yao, 2007. Frictional sliding of gabbro gouge under hydrothermal conditions, *Tectonophysics* **445**, 353 – 362, doi:10.1016/j.tecto.2007.09.008.
- Hirose, H., and K. Obara, Repeating short- and long-term slow slip events with deep tremor activity around the Bungo Channel region, southwest Japan, *Earth Planets Space*, **57**, 961-972, 2005.
- Holt, W. E., and A. J. Haines, The kinematics of northern South Island, New Zealand, determined from geologic strain rates, *J. Geophys. Res.*, **100**, 17,991-18,010, 1995.
- Houston, H., The scaling of the tremor source (abstract), *Aseismic Slip, Non-Volcanic Tremor, and Earthquakes* workshop, February 25-28, Sidney, British Columbia, 2008.
- Hyndman, R.D., and Wang, K., Thermal constraints on the zone of major thrust earthquake failure: The Cascadia Subduction Zone, *J. Geophys. Res.*, **98**, 2039-2060, (1993).
- Ide, S., G. C. Beroza, D. R. Shelly & T. Uchide, A scaling law for slow earthquakes, *Nature*, **447**, 76-79, doi:10.1038, 2007.
- Kao, H., S.-J. Shan, H. Dragert, G. Rogers, J. F. Cassidy, and K. Ramachandran (2005), A wide depth distribution of seismic tremors along the northern Cascadia margin, *Nature*, **436**(7052), 841– 844.
- Kao, H., S.-J. Shan, H. Dragert, G. Rogers, J. F. Cassidy, K. Wang, T. S. James, and K. Ramachandran (2006), Spatial-temporal patterns of seismic tremors in northern Cascadia, *J. Geophys. Res.*, **111**, B03309, doi:10.1029/2005JB003727.
- Liu, Y., Modeling moment-duration relation of aseismic slip events in subduction zones, *Aseismic Slip, Non-Volcanic Tremor, and Earthquakes* workshop, February 25-28, Sidney, British Columbia, 2008.
- Liu, Y., and Rice, J. R., Spontaneous and triggered aseismic deformation transients in a subduction fault model, *J. Geophys. Res.*, **112**, B09404, doi:10.1029/2007JB004930, (2007).
- Mao, A., C. G. A. Harrison, and T. H. Dixon, Noise in GPS coordinate time series, *J. Geophys. Res.* **104**, 2797-2816, 1999.
- Marone, C., Laboratory-derived friction laws and their application to seismic faulting, *Annual Rev. Earth Planet. Sci.* **26**, 643-696, 1998
- McCaffrey, R., DEFNODE user's guide, Rensselaer Polytechnic Institute, Troy, 1995.  
<http://www.rpi.edu/~mccaffr/defnode/>

- McCaffrey, R., Inverting 3-component GPS time series for transient sources and inter-event site velocities and fault coupling: Applications to Cascadia and Hikurangi (New Zealand) margins (abstract), *Aseismic Slip, Non-Volcanic Tremor, and Earthquakes* workshop, February 25-28, Sidney, British Columbia, 2008.
- McCaffrey, R., A. I. Qamar, R. W. King, R. Wells, G. Khazaradze, C. A. Williams, C. W. Stevens, J. J. Vollick, and P. C. Zwick, Fault locking, block rotation and crustal deformation in the Pacific Northwest, *Geophys J. Int.*, doi:10.1111/j.1365-246X.2007.03371.x, 2007.
- McCaffrey, R., L. Wallace, and J. Beavan, Slow slip and frictional transition at low temperature at the Hikurangi subduction zone, *Nature Geoscience*, in press, 2008.
- Mortimer, N., and Parkinson, D., Hikurangi Plateau; a Cretaceous large igneous province in the Southwest Pacific Ocean, *J. Geophys. Res.*, **101**, 687-696, (1996).
- Okada, Y., 1992. Internal deformation due to shear and tensile faults in a half-space, *Bull. Seismol. Soc. Amer.*, 82, 1018-1040.
- Reyners, M., Plate coupling and the hazard of large subduction thrust earthquakes at the Hikurangi subduction zone, New Zealand, *New Zealand J. Geology and Geophysics* **41**, 343-354, (1998).
- Reyners, M., and S. Bannister, Earthquakes triggered by slow slip at the plate interface in the Hikurangi subduction zone, New Zealand, *Geophys. Res. Lett.*, 34, L14305, doi:10.1029/2007GL030511, 2007
- Rothacher, M., and L. Mervart (eds.), Documentation of the Bernese GPS Software Version 4.0, 418 pp, Astron. Inst., Univ. of Bern, Bern, Switzerland, 1996.
- Schwartz, S. Y., and Rokosky, J. M., Slow slip events and seismic tremor at circum-Pacific subduction zones, *Rev. Geophys.* **45**, 2006RG000208, (2007).
- Segall, P. and M. Matthews, Time dependent inversion of geodetic data, *J. Geophys. Res.*, 102, 22,391–22,410, 1997.
- Segall, P., A. Rubin, and J. R. Rice, Dilatancy stabilization of frictional sliding as a mechanism for slow slip events, (abstract), *Aseismic Slip, Non-Volcanic Tremor, and Earthquakes* workshop, February 25-28, Sidney, British Columbia, 2008.
- Segall, P., and J. R. Rice, Dilatancy, compaction, and slip instability of a fluid-infiltrated fault, *J. Geophys. Res.*, 100, 22155-22171, 1995.
- Segall, P., E. K. Desmarais, D. R. Shelly, A. Miklius, and P. Cervelli (2006), Earthquakes triggered by silent slip events on Kilauea volcano, Hawaii, *Nature*, 442(7098), 71– 74.
- Shelly, D. R., G. C. Beroza, S. Ide, and S. Nakamura (2006), Low frequency earthquakes in Shikoku, Japan, and their relationship to episodic tremor and slip, *Nature*, 442(7099), 188– 191.
- Sibson, R. H., and J. V. Rowland, Stress, fluid pressure and structural permeability in seismogenic crust, North Island, New Zealand, *Geophys. J. Int.*, 154, 584-594, 2003.
- Tichelaar, B. W., and L. J. Ruff, Depth of seismic coupling along subduction zones, *J. Geophys. Res.*, 98, 2017-2037, 1993.
- Villamor, P., and K. Berryman, A late Quaternary extension rate in the Taupo Volcanic Zone, New Zealand, derived from fault slip data. *New Zealand Journal of Geology and Geophysics* 44: 243–269, 2000.
- Walcott, R. I., The kinematics of the plate boundary zone through New Zealand: A comparison of short- and long-term deformations, *Geophys. J. R. Astron. Soc.*, 79, 613-633, 1984.

- Walcott, R. I., 1978. Geodetic strains and large earthquakes in the axial tectonic belt of North Island, New Zealand, *J. geophys. Res.*, **83**, 4419–4429.
- Wallace, L. M., and Beavan, J., A large slow slip event on the central Hikurangi subduction interface beneath the Manawatu region, North Island, New Zealand, *Geophys. Res. Lett.* **33**, L11301, doi:10.1029/2006GL026006, (2006).
- Wallace, L. M., Beavan, J., McCaffrey, R., and Darby, D., Subduction zone coupling and tectonic block rotations in the North Island, New Zealand, *J. Geophys. Res.*, **109**, B12406, doi:10.1029/2004JB003241, (2004).
- Wallace, L. M., Beavan, J., McCaffrey, R., & Berryman, K., 2006. Balancing the plate motion budget in the South Island, New Zealand using GPS, geological and seismological data, , *Geophysical Journal International*, , doi:10.1111/j.1365-246X.2006.03183.x.
- Wang, K., Wells, R., Mazzotti, S., Hyndman, R. D., and Sagiya, T., A revised dislocation model of interseismic deformation of the Cascadia subduction zone, *J. Geophys. Res.*, **108**, 2026, doi:10.1029/2001JB001227, (2003).
- Webb, T.H. and Anderson, H., 1998. Focal mechanisms of large earthquakes in the North Island of New Zealand: strain partitioning at an oblique active margin, *Geophys. J. Int.*, **134**, 40–86.
- Wellman, H. W., Recent crustal movements in New Zealand, *Tectonophysics*, 23, 423-24, 1974.
- Wilson, C. J. N.; Houghton, B. F.; McWilliams, M. O.; Lanphere, M. A.; Weaver, S. D.; Briggs, R. M., Volcanic and structural evolution of the Taupo Volcanic Zone, New Zealand: a review. *Journal of Volcanology and Geothermal Research* 68: 1–28, 1995.

## Figures

Figure 1. (a) Physiographic map of New Zealand region. Arrows show convergence of Pacific relative to Australia (Beavan et al., 2002). Box shows area of Fig. 1b. (b) Red and blue dots show locations of continuous GPS sites (red are used in this study; blue are not used due to short operating times). Dashed curves are depth contours of top of subducting Pacific plate labeled in km. Black dots show the spacing of grid points used to define the plate interface.

Figure 2. Gaussian form of the slow-slip time functions. The free parameters are the center time  $T_c$  and the spread  $T_s$ . Dashed line is to simulate accelerated locking that appears to follow some slip events.

Figure 3. Examples of time series and fits. Amplitude scale has had linear velocity removed. Gray curves show model predictions and triangles show where slip events produce > 1 mm of slip at the site. Triangles at bottom show start times of the slip events. Asterisks mark where accelerated re-loading may be occurring following slow-slip.

Figure 4. Maps of slip distributions and surface displacements for selected events. Red vectors are horizontal displacements, brown are vertical. Dashed lines are fault depth contours (at 3, 15, 30, 50, 70 and 90 km). Red dots are cGPS sites operating at the time of the event. Gray triangles are volcanoes.

Figure 5. Map of total fault slip (colored contours) and total surface displacements at sites resulting from all slow slip events. Red vectors show horizontal displacements and brown vectors are vertical. Dashed lines are fault depth contours as labeled in km.

Figure 6. (a) Site velocity vectors. Blue are velocities corrected for slow-slip (velocities between events) and red are average velocities (uncorrected for slow slip). (b) Map of locked zone from uncorrected (average) surface velocities. Purple vectors are observed and blue are calculated. Red curves are the total fault slip contours from slow-slip; contours are 100 mm starting at 50 mm. (c) Locking distribution derived from corrected vectors (velocities between slip events) and slow-slip contours as in Fig. 6b.

Figure 7. Log-log plot of the duration v. moment of Hikurangi slow slip events (numbered circles) and others from subduction zones (compilation from Schwartz and Rokosky, 2007). Shallow events

are those less than about 25 km. The blue lines show relationships where moment is proportional to duration and to duration to the 0.7 power, as suggested by Schwartz and Rokosky (2007).

Supplemental Material: All time series with fits, residuals, individual event maps, corrected and uncorrected velocities.

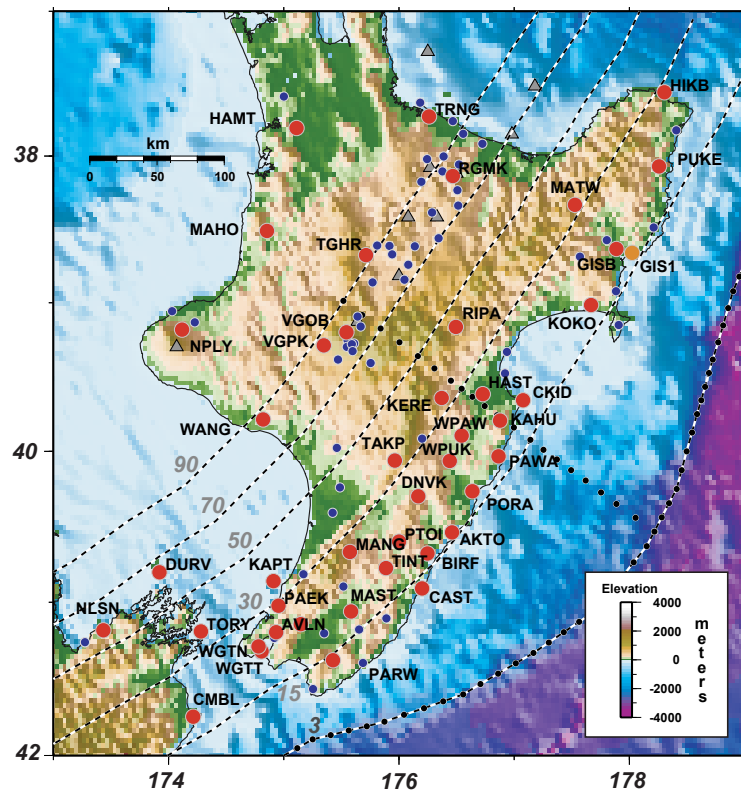
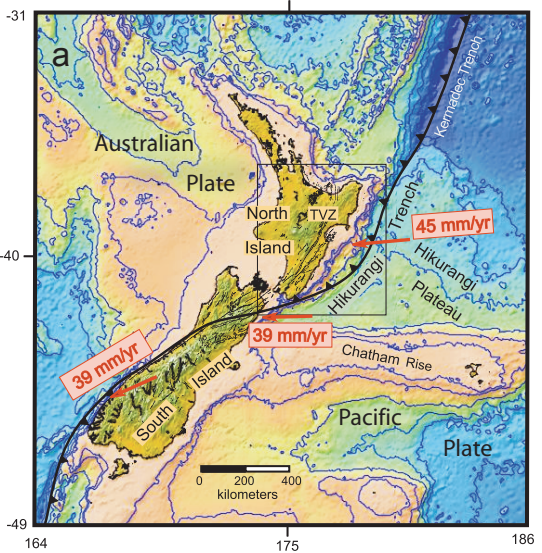
Table 1. Slow-slip event parameters and formal uncertainties.

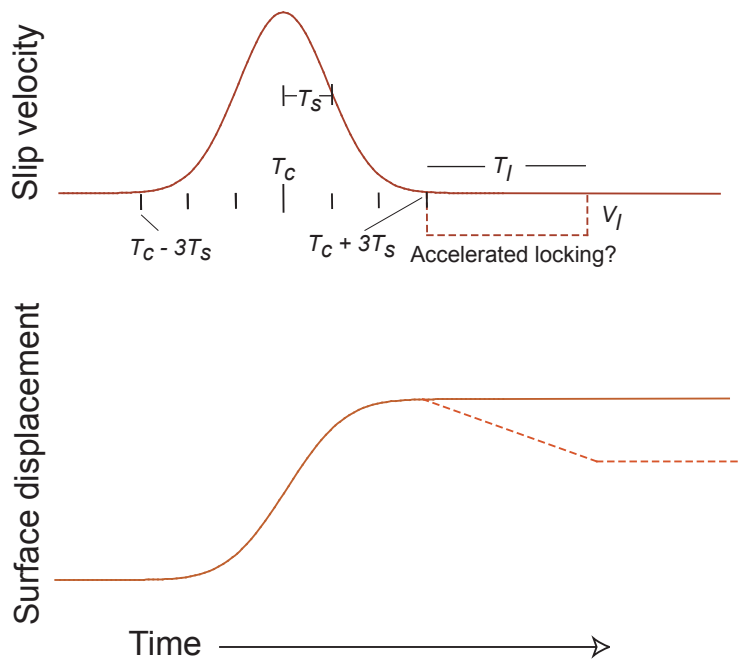
Event	Date	Longitude, °E	$\sigma$ , °E	Latitude, °S	$\sigma$ , °S	X,, km	$\sigma$ , km	W,, km	$\sigma$ , km	A, mm/yr	$\sigma$ , mm/yr
1	20021003	178.35	0.06	-38.85	0.01	13.9	5.6	9.2	4.0	406	44
2	20021105	174.59	0.02	-40.97	0.01	28.8	1.2	11.4	1.9	250	37
3	20030122	178.35	0.07	-38.90	0.03	7.3	9.8	14.3	10.1	91	119
4	20030817	177.23	0.40	-39.75	0.22	15.0	19.7	8.0	50.1	98	480
5	20040213	175.46	0.04	-40.11	0.03	4.7	10.0	14.4	4.4	376	691
6	20040507	177.23	0.40	-39.75	0.22	15.0	19.7	8.0	50.1	96	470
7	20040712	175.60	0.01	-40.13	0.00	34.4	0.6	12.0	0.6	539	26
8	20041019	178.35	0.07	-38.90	0.03	19.5	3.3	14.9	5.0	215	40
9	20050620	178.35	0.07	-38.90	0.03	3.0	112.7	8.8	21.0	87	933
10	20060127	178.35	0.07	-38.90	0.03	34.9	4.6	5.7	20.3	87	311
11	20060520	177.62	0.07	-40.06	0.05	25.3	2.7	14.8	7.5	185	88
12	20060603	177.96	0.01	-38.82	0.02	35.0	2.5	5.7	1.1	112	18
13	20060819	177.26	0.01	-40.25	0.01	27.5	0.6	6.4	2.9	449	205

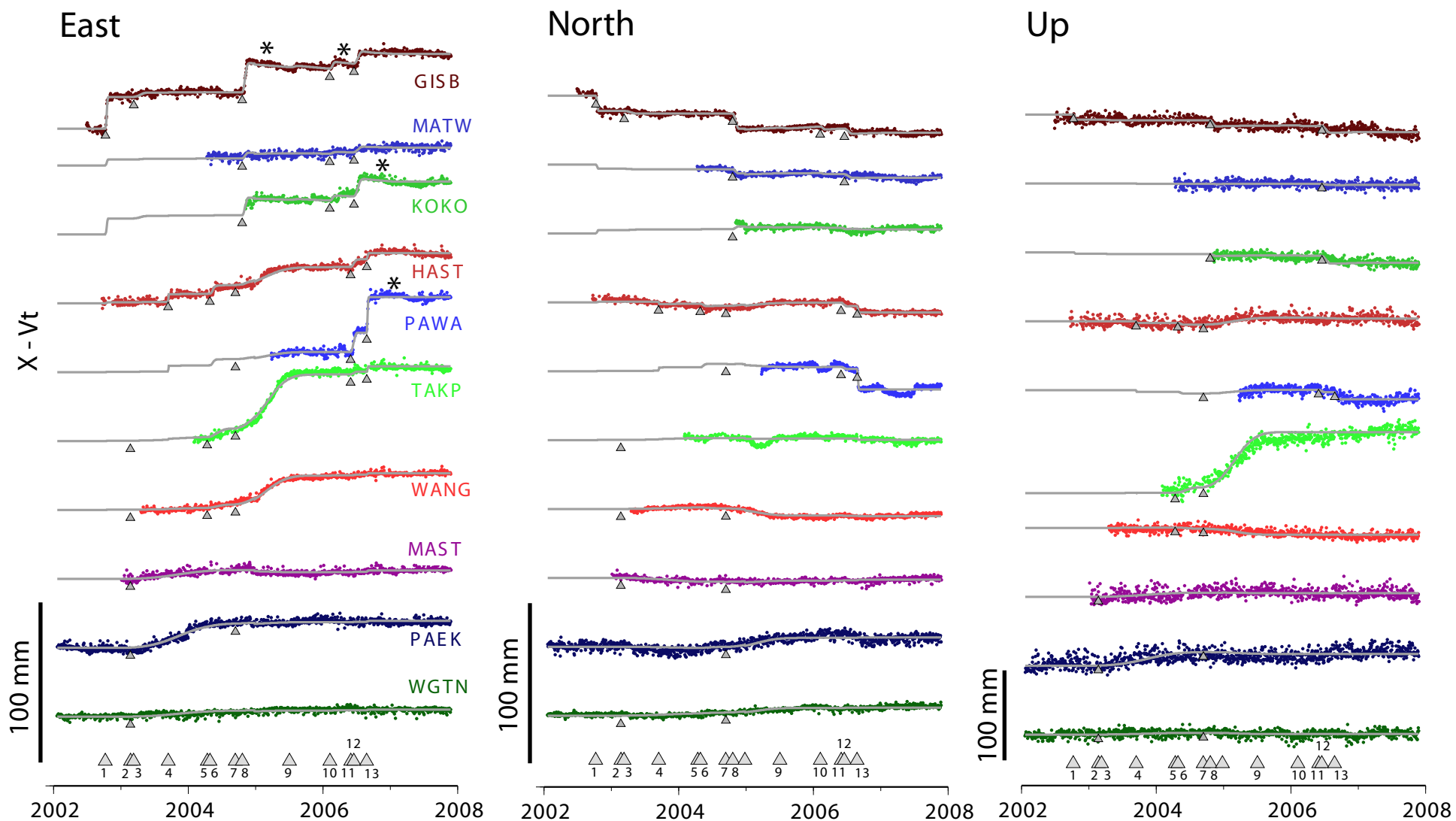
Table 1 (continued)

Event	$T_c$ , years	$\sigma$ , years	$T_s$ , days	$\sigma$ , days	$V_1$	$\sigma$	$T_b$ , days	$\sigma$ , days	Slip, mm	Area, km <sup>2</sup>	$M_o$ , Nm	Slip over length	Mo/time, N-m/day	
1	2002.756	0.003	3.9	0.3					6.67	120	2613	1.26E+19	2.35E-06	9.36E+12
2	2002.844	0.038	123.7	4.4					6.82	71	7553	2.16E+19	8.17E-07	5.05E+11
3	2003.058	0.015	23.0	0.0					6.18	24	2381	2.33E+18	4.92E-07	2.93E+11
4	2003.626	0.031	9.4	3.8					6.24	25	2889	2.90E+18	4.65E-07	8.92E+11
5	2004.120	0.066	41.5	8.3					6.48	95	1735	6.61E+18	2.28E-06	4.61E+11
6	2004.347	0.017	2.9	2.0					6.24	24	2889	2.84E+18	4.47E-07	2.84E+12
7	2004.528	0.015	79.8	1.6					7.11	160	8933	5.72E+19	1.69E-06	2.08E+12
8	2004.798	0.005	6.0	0.6	64	15	276	18	6.72	66	5719	1.53E+19	8.73E-07	7.37E+12
9	2005.469	0.000	1.0	8.6					5.88	20	987	8.29E+17	6.37E-07	2.4E+12
10	2006.072	0.000	7.5	0.8					6.35	24	4342	4.26E+18	3.64E-07	1.64E+12
11	2006.385	0.007	9.0	0.9					6.76	57	7563	1.73E+19	6.55E-07	5.56E+12
12	2006.423	0.000	11.8	0.4	41	13	154	28	6.43	30	4541	5.53E+18	4.45E-07	1.36E+12
13	2006.634	0.002	3.5	0.3					6.79	115	4171	1.92E+19	1.78E-06	1.59E+13

Columns labeled  $\sigma$  give the standard error for the parameter in the preceding column. The total event duration is approximately 4 times  $T_s$ .







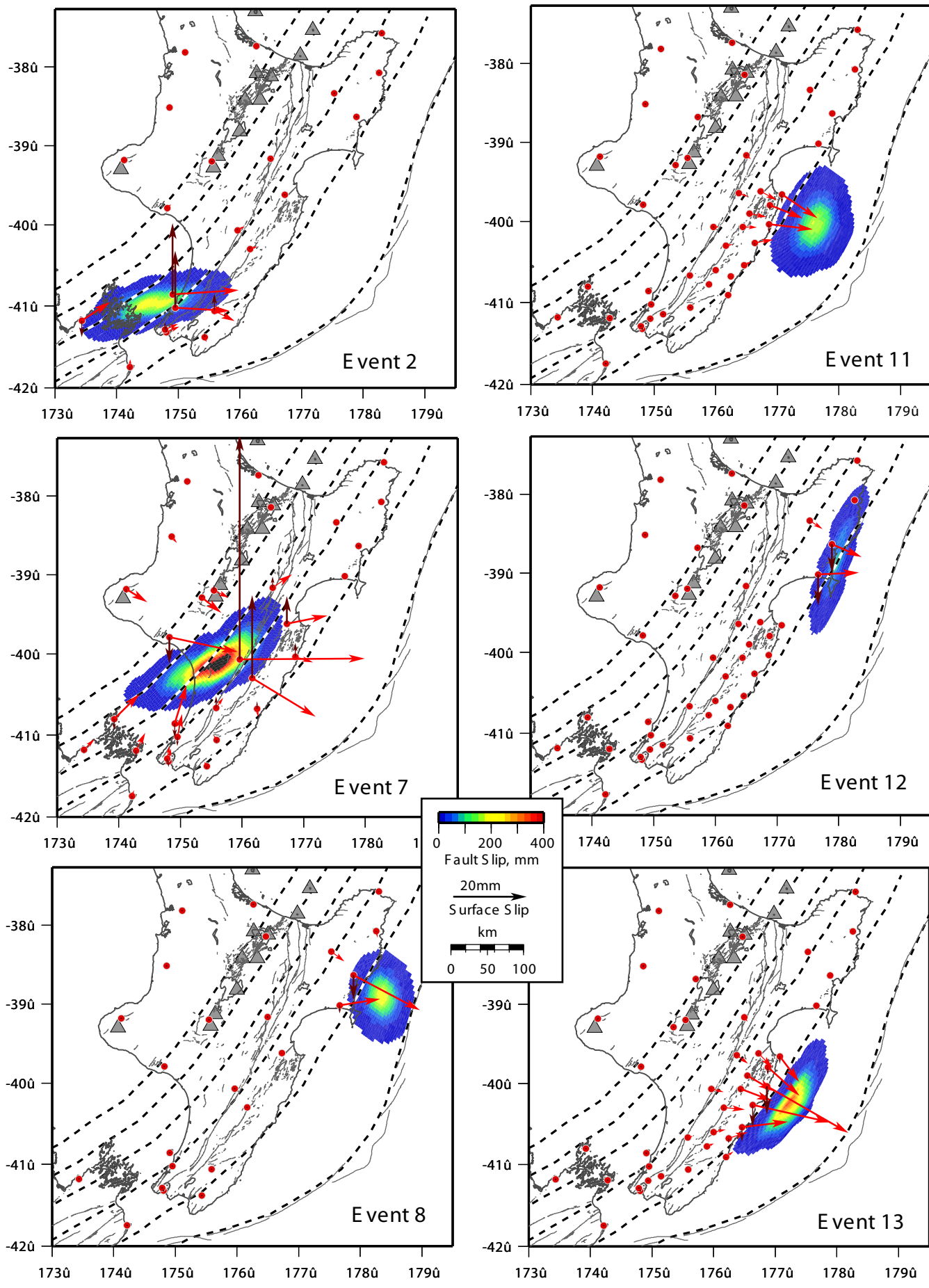


Figure 4

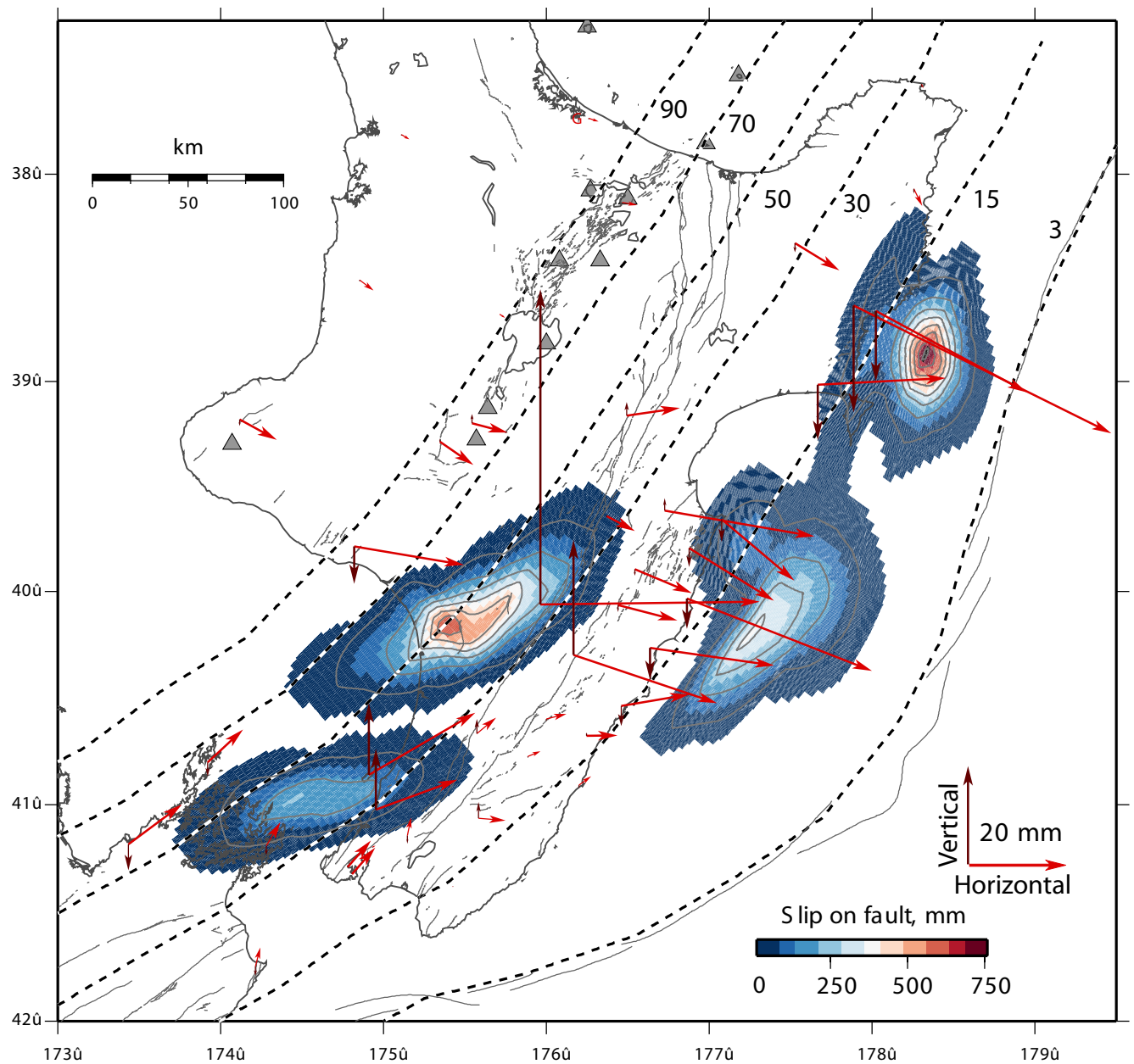


Figure 5

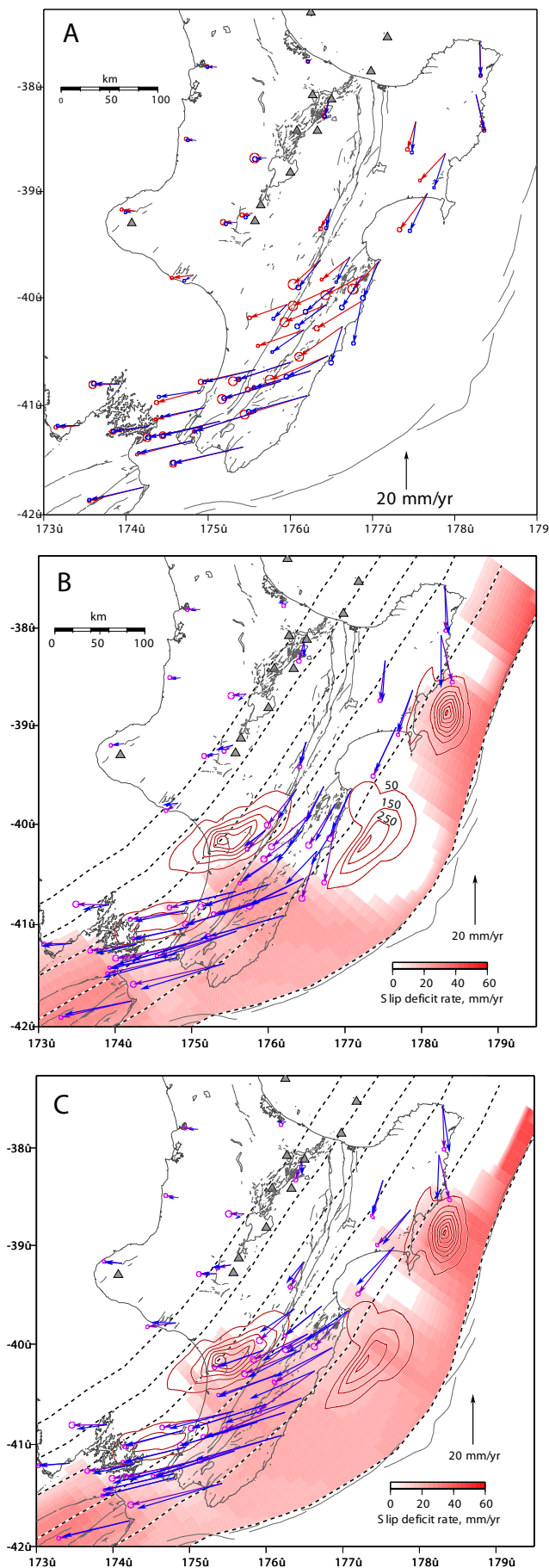


Figure 6

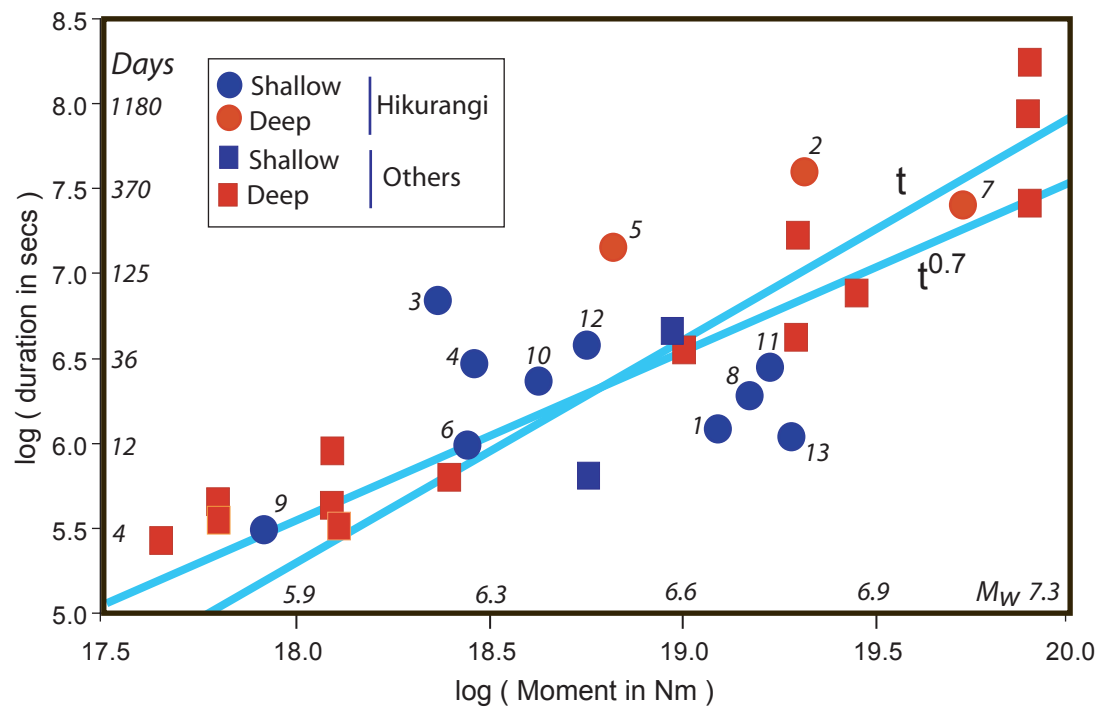


Figure 7